Photometric Stereo under Perspective Projection

Ariel Tankus
School of Computer Science
Faculty of Exact Sciences
Tel-Aviv University
Tel-Aviv, 69978
arielt@post.tau.ac.il

Nahum Kiryati
Department of Electrical Engineering–Systems
Faculty of Engineering
Tel-Aviv University
Tel-Aviv, 69978
nk@eng.tau.ac.il

Abstract

Photometric stereo is a fundamental approach in Computer Vision. At its core lies a set of image irradiance equations each taken with a different illumination. The vast majority of studies in this field have assumed orthography as the projection model. This paper re-examines the basic set of equations of photometric stereo, under an assumption of perspective projection. We show that the resulting system is linear (as is the case under the orthographic model; Nevertheless, the unknowns are different in the perspective case). We then suggest a simple reconstruction algorithm based on the perspective formulae, and compare it to its orthographic counterpart on synthetic as well as real images. This algorithm obtained lower error rates than the orthographic one in all of the error measures. These findings strengthen the hypothesis that a more realistic set of assumptions, the perspective one, improves reconstruction significantly.

1. Introduction

Photometric stereo is a monocular 3D shape reconstruction method based on several images of a scene taken from an identical viewpoint under different illumination conditions. The most common approach in the field, first introduced by Woodham in the 1970s [24], [25], divides the task into two: recovery of surface gradients and integration of the resultant gradient field to determine the 3D surface. The goal of the first part is to solve a system of equations, each of which represents the relation of one reflectance map to its corresponding image intensity and is known as an image irradiance equation. The vast majority of works in the field add simplifying assumptions to the set of equations. Of particular importance is the common assumption that scene points are projected orthographically during the photographic process.

*This research has been supported in part by Tel-Aviv University fund, the Adams Super-Center for Brain Studies, the Israeli Ministry of Science, the ISF Center for Excellence in Applied Geometry, and the A.M.N. fund.

Many works in the field of photometric stereo have followed the seminal work of Woodham [24], [25], and assumed orthographic projection. Some early examples are [9], [23], [17], [8]. The more recent approach of Kim and Park [11] represents the 3D surface by Legendre polynomials, linearizes the reflectance map and minimizes an energy functional. Works on uniqueness in photometric stereo are those of Kozera [12] and Okatani and Deguchi [16]. Noakes and Kozera [15] employ the 2D Leap-Frog scheme for solving the photometric stereo problem and prove its convergence to the maximum-likelihood surface estimate given a suitable initial guess. Iwahori et al. [10] employ neural networks for photometric stereo. Yuille et al. [26] learn generative models of objects from images with different, unknown illuminations. These models can approximate object appearance under a range of lighting conditions. Ref. [6] presents a method for bias correction in photometric stereo using control points. These are only a few of the many works in the field of photometric stereo which employ the orthographic projection model. Photometric stereo was also considered with other conditions such as non-Lambertian surfaces [7] and [20], four light sources with color images [1] or lights which are isotropic and distant from the object but otherwise unconstrained [2]; we shall not deal with these configurations in this paper.

Despite the large amount of literature in the field, only two works on photometric stereo (the authors know of) relate to perspective projection. The first is that of Lee and Kuo [13]. Their goal is to combine photometric stereo and geometric stereo cues. This work, however, employs an approximation of the depth function expressed as a linear combination of individual element basis functions. The approximated equations are then combined with geometric stereo cues, and solved by minimization of an energy functional. Thus, the image irradiance equations formulated under the perspective projection model ([22], [18], [3]) are unused.

The other perspective method is that of Galo and Tozzi [4]. Their work differs from the current one by

two significant aspects. First, it assumes proximate light sources, whereas ours assumes infinitely distant ones. The second and most important is that the set of equations in [4] has mixed parameters: some parameters are in image coordinates and some, in real-world coordinates. As [4] does not employ the perspective image irradiance equation ([22], [18], [3]), which expresses the reflectance map—intensity relation in image coordinates only, they need to approximate the equations using Taylor series, which they solve using iterations. The important point is that when mixed coordinates are used, even if one recovers depth derivatives correctly in real-world coordinates, one cannot directly integrate them, as the real-world grid is unknown (only the image grid is known and uniform).

While the vast majority of the photometric stereo literature assumes orthographic projection, and the two existing perspective-projection studies use an approximation-based approach, no information is available on the accurate solution of a set of image irradiance equations under the perspective projection model. The goal of this research was to re-examine the fundamental system of equations of photometric stereo based on the more realistic, perspective projection.

As [22] and [18] show, the perspective image irradiance equation depends on the directional derivatives of the natural logarithm of the depth function with respect to image coordinates (we denote these derivatives p and q). We therefore derive a closed form solution to a system of 3 perspective equations with the 3 unknowns p, q, and ρ, where ρ is the albedo. We show that the system of equations remains linear under the perspective case as well (cf. [25]), and that its solution is a generalization of the orthographic solution. We compare reconstruction by the perspective photometric stereo and by the orthographic one.

The paper is organized as follows. Following the presentation of notation and basic assumptions (Sect. 2), we briefly introduce the image irradiance equations under the perspective projection model (Sect. 3). Section 4 then develops the solution to a set of three image irradiance equations under the perspective projection model. Section 5 uses the solution as a part of an algorithm for solving the photometric stereo problem under perspective projection. Section 6 compares of the algorithm with its orthographic counterpart on synthetic and real images. Finally, Sect. 7 draws the conclusions.

2. Notation and Assumptions

The following notation and assumptions hold throughout this paper. Photographed surfaces are assumed representable by functions of world coordinates as well as of image coordinates. $\hat{z}(x,y)$ denotes the depth function in a world Cartesian coordinate system whose origin is at camera plane. If the real coordinate $(x,y,\hat{z}(x,y))$ is projected onto image point (u,v), then its depth is denoted $z(u,v)$. By definition, $z(u,v)=\hat{z}(x,y)$. f denotes the focal length, and is assumed known. The scene is Lambertian, and is illuminated from directions $\vec{L}_i=(p_{s_i},q_{s_i},-1)$ (where $i=1,2,3$) by a point light source at infinity. $\vec{N}(x,y)$ is the surface normal. $\hat{\rho}(x,y)$ denotes the albedo at point $(x,y,\hat{z}(x,y))$, and $\rho(u,v)$ is the albedo projected onto image point (u,v). By definition, if point $(x,y,\hat{z}(x,y))$ is projected onto image point (u,v), then $\hat{\rho}(x,y)=\rho(u,v)$.

3. Background: The Image Irradiance Equation in Image Coordinates

Let us first introduce the image irradiance equation (see [5]) under perspective projection. This was first presented by [21], [18].

In its general form, the image irradiance equation [5] is:

$$I(u,v)=\hat{\rho}(x,y)\frac{\vec{L}\cdot\vec{N}(x,y)}{\|\vec{L}\|\|\vec{N}(x,y)\|} \tag{1}$$

Under the perspective projection model, the following relation between image coordinates (u,v) and real-world coordinates $(x,y,\hat{z}(x,y))$ holds:

$$x=-\frac{u\cdot\widehat{z}(x,y)}{f};\qquad y=-\frac{v\cdot\widehat{z}(x,y)}{f}$$

Under this model, Eq. 1 can be expressed as a function of image coordinates only, which results in ([21], [18]):

$$I(u,v)=\rho(u,v)\frac{(u-fp_s)z_u+(v-fq_s)z_v+z}{\|\vec{L}\|\sqrt{(uz_u+vz_v+z)^2+f^2(z_u^2+z_v^2)}} \tag{2}$$

where $z(u,v)\stackrel{def}{=}\widehat{z}(x,y)$ for (u,v) which is the perspective projection of $(x,y,\widehat{z}(x,y))$. Equation 2 is the *perspective image irradiance equation*.

Another way to express Eq. 2:

$$I(u,v)=\rho(u,v)\frac{(u-fp_s)p+(v-fq_s)q+1}{\|\vec{L}\|\sqrt{(up+vq+1)^2+f^2(p^2+q^2)}} \tag{3}$$

where $p\stackrel{def}{=}\frac{z_u}{z}=\frac{\partial\ln z}{\partial u}$ and $q\stackrel{def}{=}\frac{z_v}{z}=\frac{\partial\ln z}{\partial v}$. Eq. 3 depends on the derivatives of $\ln(z(u,v))$, but not on $\ln(z(u,v))$ itself. Because the natural logarithm is a bijective mapping and $z(u,v)>0$, the problem of recovering $z(u,v)$ from the image irradiance equation reduces to the problem of recovering the surface $\ln(z(u,v))$ from Eq. 3.

4. Perspective Photometric Stereo

Photometric stereo employs several images of the same object from an identical viewpoint under different illumina-

tions. We denote the images $\{I_i(u,v)\}_{i=0}^{n-1}$ and the corresponding illuminations $\{\vec{L}_i\}_{i=0}^{n-1}$. The perspective image irradiance equations are:

$$I_i(u,v) = \rho(u,v)\frac{(u-fp_{s_i})p+(v-fq_{s_i})q+1}{\|\vec{L}_i\|\sqrt{(up+vq+1)^2+f^2(p^2+q^2)}}$$

Dividing the i^{th} image by the k^{th} (assuming the k^{th} is non-zero everywhere) yields:

$$\frac{I_i(u,v)}{I_k(u,v)} = \frac{\|\vec{L}_k\|((u-fp_{s_i})p+(v-fq_{s_i})q+1)}{\|\vec{L}_i\|((u-fp_{s_k})p+(v-fq_{s_k})q+1)}$$

which can be written as:

$$A_{ik}p+B_{ik}q+C_{ik}=0 \tag{4}$$

where:

$$\begin{aligned} A_{ik} &= I_i(u,v)\|\vec{L}_i\|(u-fp_{s_k}) - I_k(u,v)\|\vec{L}_k\|(u-fp_{s_i}) \\ B_{ik} &= I_i(u,v)\|\vec{L}_i\|(v-fq_{s_k}) - I_k(u,v)\|\vec{L}_k\|(v-fq_{s_i}) \\ C_{ik} &= I_i(u,v)\|\vec{L}_i\| - I_k(u,v)\|\vec{L}_k\| \end{aligned}$$

Thus, we have 3 unknowns (p, q, and ρ). As the system of equations is linear also in the perspective case (cf. [25] for the orthographic case), 3 images are enough to recover the unknowns in the general case. We obtain:

$$p = \frac{I_0\|\vec{L}_0\|\Delta q_s^{21} + I_1\|\vec{L}_1\|\Delta q_s^{02} + I_2\|\vec{L}_2\|\Delta q_s^{10}}{I_0\|\vec{L}_0\|D_{12} + I_1\|\vec{L}_1\|D_{20} + I_2\|\vec{L}_2\|D_{01}} \tag{5}$$

$$q = \frac{I_0\|\vec{L}_0\|\Delta p_s^{12} + I_1\|\vec{L}_1\|\Delta p_s^{20} + I_2\|\vec{L}_2\|\Delta p_s^{01}}{I_0\|\vec{L}_0\|D_{12} + I_1\|\vec{L}_1\|D_{20} + I_2\|\vec{L}_2\|D_{01}} \tag{6}$$

where: $\Delta p_s^{ik} = p_{s_i} - p_{s_k}$, $\Delta q_s^{ik} = q_{s_i} - q_{s_k}$ and

$$D_{ik} = u(q_{s_i} - q_{s_k}) + v(p_{s_k} - p_{s_i}) + f(p_{s_i}q_{s_k} - p_{s_k}q_{s_i})$$

$i,k = 0,1,2$. ρ is obtained by substitution of the above p and q into one of the image irradiance equations.

Eqs. 5, 6 are exact solutions of Eq. 4 for ideal images. In the presence of image noise, however, a non-linear optimization procedure (e.g., Levenberg-Marquardt) may be preferred. In an ideal environment, the solution gradients p and q (Eqs. 5, 6) are integrable due to their uniqueness.

4.1. Generalization of Orthographic Photometric Stereo

Let us denote $\hat{p}$, $\hat{q}$ the x- and y-derivatives of $\hat{z}(x,y)$. In the orthographic case, the well known image irradiance equations are

$$I_i(x,y) = \hat{\rho}(x,y)\frac{p_{s_i}\hat{p}+q_{s_i}\hat{q}+1}{\|\vec{L}_i\|\sqrt{\hat{p}^2+\hat{q}^2+1}}$$

$i = 0,1,2$. The solution of this system of equation is given by:

$$\hat{p} = \frac{I_0\|\vec{L}_0\|\Delta q_s^{12} + I_1\|\vec{L}_1\|\Delta q_s^{20} + I_2\|\vec{L}_2\|\Delta q_s^{01}}{I_0\|\vec{L}_0\|E_{12} + I_1\|\vec{L}_1\|E_{20} + I_2\|\vec{L}_2\|E_{01}} \tag{7}$$

$$\hat{q} = \frac{I_0\|\vec{L}_0\|\Delta p_s^{21} + I_1\|\vec{L}_1\|\Delta p_s^{02} + I_2\|\vec{L}_2\|\Delta p_s^{10}}{I_0\|\vec{L}_0\|E_{12} + I_1\|\vec{L}_1\|E_{20} + I_2\|\vec{L}_2\|E_{01}} \tag{8}$$

where $E_{ik} = p_{s_i}q_{s_k} - p_{s_k}q_{s_i} i, k = 0,1,2$. It can be shown that the solution of the perspective set of equations (Eq. 5, 6) generalizes the orthographic solution (Eq. 7, 8) when $f \to \infty$ (in which case also: $u \to x$ and $v \to y$). The proof is omitted for brevity.

5. The Algorithm

For perspective photometric stereo we suggest the direct use of Eqs. 5, 6 to recover the derivatives p and q. For the numerical integration part we employed the Gauss-Seidel iterative scheme (see [19] for a review of the scheme). Ref. [6] details the equations of numerical integration for the photometric stereo case under the orthographic model. The same integration procedure is applied to the perspective case, but now the inputs are p and q rather than $\hat{p}$ and $\hat{q}$ (i.e., derivatives of the natural logarithm of the depth, rather than of the depth itself). Therefore, the perspective algorithm has an additional stage of taking the exponent of the result of the integration.

6. Experimental Results

6.1. The Experiments

This section describes experiments conducted with the suggested algorithm for photometric stereo. To evaluate the contribution of perspective photometric stereo, we juxtaposed it with a similar algorithm based on the orthographic equations (Eqs. 7, 8). Both solutions of the perspective and orthographic systems of equations were then integrated by the Gauss-Seidel scheme (the same code was used for both methods; 10,000 iterations). For the perspective one, an exponent of the result was then taken.

We selected the simple orthographic algorithm, because its numerical scheme is identical to ours, so any improvement in results can be attributed to the change of equations.

Because this paper is not concerned with runtime issues but rather with the underlying photometric equations, the Gauss-Seidel scheme was applied as one of the simplest iterative schemes. See [6] for a detailed runtime comparison of iterative schemes utilized for photometric stereo. The runtime complexity of perspective photometric stereo is identical to that of the orthographic method.

We evaluated the performance of the algorithms by comparing the reconstructed surfaces with their corresponding

originals according to three criteria (described below). The synthetic images in the comparison were produced from an original surface $\widehat{z}(x,y)$ in the manner described in [22]. The real images were photographed by a Canon PowerShot G5 camera with aperture size, exposure time and white balance set to fixed values manually (and flash disabled). The illumination direction was measured according to the sundial principal (see [6] for details). The illuminator was a standard 500W rectangular projector. The object was a plastic mannequin head, whose true 3D shape was acquired in advance using a high precision Cyberware laser-based range scanner. We did not process the eyes in the images, due to their specularity.

The error measures employed in the comparison of a reconstructed surface with the original one were adopted from Shah et al. [27]: the mean and standard deviation of the depth error and the mean gradient error. The calculation of the error rates was achieved via the Moving Least Squares method [14], as described in [22].

For the real example, the calculation of error measures required an additional step, because scanning was done prior to the photometric stereo experiments (unrepeatable in our lab), so subject pose during photography differed from that of the ground truth. Registration was accomplished by translation of the mouth centers of all surfaces (marked manually) to the origin, scaling based on a size measurement of the object and manually approximate a rotation of the model at the time of scanning to its pose at the time of photography (10^o around the x-axis CCW). This step clearly reduced the discrepancy between orthographic and perspective reconstructions, thus partially compensating the flaws of the orthographic one.

6.2. Comparative Evaluation

The synthetic surfaces we considered were $\hat{z}(x,y) = 2\cos(\sqrt{(x-1)^2+(y-2)^2})+10$ and $\hat{z}(x,y) = \sin(3(x+y))+15$. Fig. 1 presents the synthetic images for the cosine example along with the original surface and the orthographic and perspective reconstructions (Similar figures for the sine example[1] are omitted due to lack of space). The figure shows that orthographic reconstruction managed to recover the dome-shaped part of the surface, but for the descending part (outside the "dome", at the negative y values) the depth of the reconstructed surface was too low comparing to the original. Perspective photometric stereo reconstructed the surface much more accurately.

Table 1A,B presents the error measures in the reconstruction of the two surfaces by each of the algorithms. According to all measures (except for mean depth error for the sine surface), surfaces reconstructed by perspective photometric stereo were significantly closer to the original than those recovered orthographically.

[1] $x,y \in [-3.1174, 3.1079]$, light source directions: $\vec{L}_0 = (0.15,-0.15,-1)$, $\vec{L}_1 = (-0.15,0.15,-1)$, $\vec{L}_2 = (-0.15,-0.15,-1)$, focal length: $f = 2$.

	Alg.:	Mean Depth Error:	Std. Dev. Depth Error:	Mean Gradient Error:
A.	Orth.:	0.10	0.14	0.07
	Pers.:	0.07	0.05	0.06
B.	Orth.:	0.15	0.11	0.47
	Pers.:	0.15	0.10	0.17
C.	Orth.:	0.72	0.87	107.03
	Pers.:	0.67	0.79	8.73

Table 1: Errors in reconstruction. **A.** $\widehat{z}(x,y) = 2\cos(\sqrt{(x-1)^2+(y-2)^2})+10$. **B.** $\hat{z}(x,y) = \sin(3(x+y))+15$. **C.** Mannequin head.

Figure 2 presents the original images (A, B, C), original surface (D) and reconstructions of the mannequin head (E, F). In Fig. 2E,F, we see the orthographic projection of the two reconstructed surfaces onto plane $[xy]$ (rendered as surfaces). Pay special attention to the projection of the lower image boundary of the reconstructed surfaces. The orthographic algorithm reconstructed a surface whose orthographic projection onto plane $[xy]$ is linear and parallel to the x axis. This implies that the boundary of the reconstructed surface lies in a plane parallel to plane $[xz]$. However, the original images were taken by a camera whose projection is close to perspective. This means the projection lied on the plane through the row of image pixels and the center of projection, which is not parallel to plane $[xz]$. As a result, according to the orthographic reconstruction, the original surface should be a line parallel to plane $[xz]$ (the intersection of two planes). The mannequin head certainly has no such straight lines. Perspective photometric stereo recovered a convex boundary, which fits the object better.

Table 1C presents the error measures in the reconstruction of the mannequin head by each of the algorithms. Perspective photometric stereo performed better according to all error measures. An important point regarding the quantization of the error for the real example is the registration of the reconstructed surfaces and the scanned one, which involved a similarity transformation. This transformation might have reduced the differences between orthographic and perspective reconstructions.

7. Conclusions

This research re-examined the core of the field of photometric stereo, the set of image irradiance equations taken under varying illumination conditions. We showed the system of equations is linear in p, q (the derivatives of the natural logarithm of the depth function with respect to image coordi-

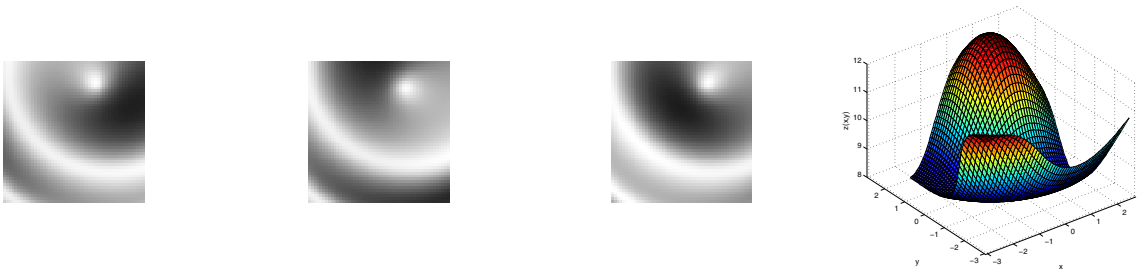

Original image: $\vec{L}_0 = (0.25, -0.25, -1)$ | Original image: $\vec{L}_1 = (-0.25, 0.25, -1)$ | Original image: $\vec{L}_2 = (-0.25, -0.25, -1)$ | Original surface.

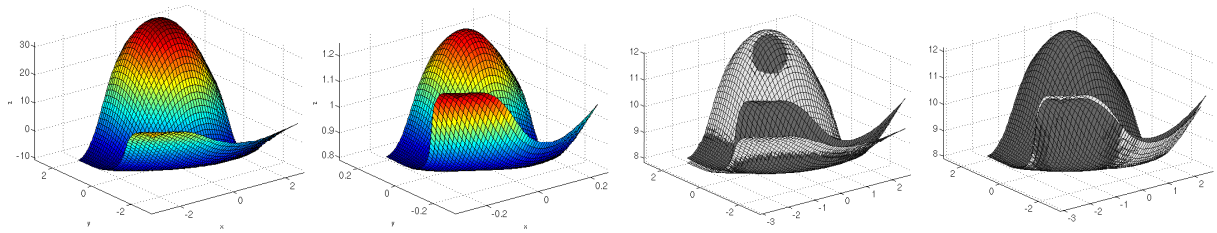

Orthographic reconstruction. | Perspective reconstruction. | Orthographic vs. original. | Perspective vs. original.

Figure 1: The synthetic surface: $\widehat{z}(x,y) = 2\cos(\sqrt{(x-1)^2+(y-2)^2}) + 10$ ($x \in [-3.0784, 2.7278]$, $y \in [-3.0792, 2.8893]$). **Top row:** Original images (below is the corresponding light source direction; focal length $f = 0.5$) and the original surface. **Bottom row:** The surfaces reconstructed by the orthographic and perspective methods, and the same reconstructions overlaid on the original surface (dark=original surface; bright=reconstructed).

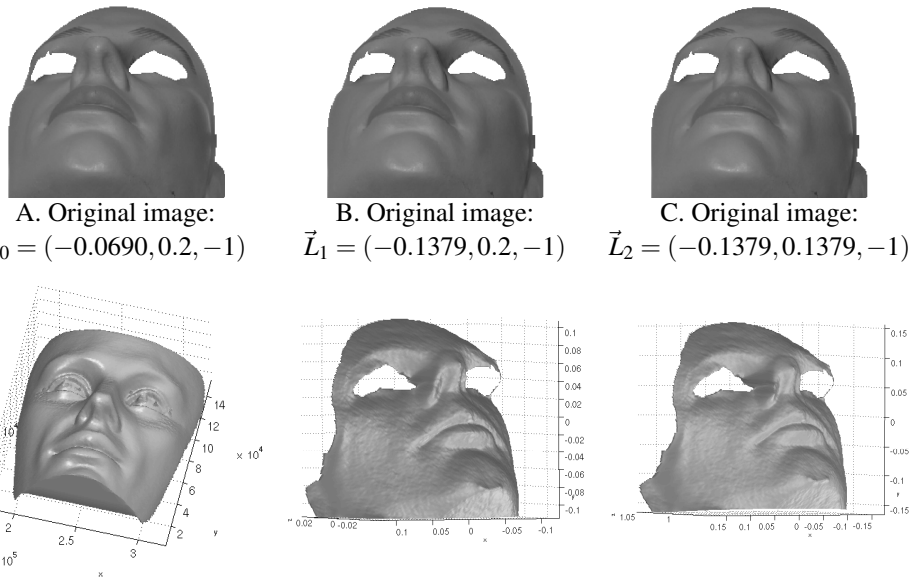

A. Original image: $\vec{L}_0 = (-0.0690, 0.2, -1)$ | B. Original image: $\vec{L}_1 = (-0.1379, 0.2, -1)$ | C. Original image: $\vec{L}_2 = (-0.1379, 0.1379, -1)$

D. Rendered ground truth. | E. Orthographic reconstruction. | F. Perspective reconstruction.

Figure 2: A real example: mannequin head. **(A), (B), (C):** Original images with background and eye regions removed. Below each image is the corresponding light source direction measured according to the sundial principal. **(D):** The original surface. Its true 3D shape was obtained by a laser scanner. **(E), (F):** The surfaces reconstructed by the orthographic and perspective methods, respectively. For the presentation, all surfaces were rendered with illumination $\vec{L} = (0.2, -0.2, -1)$.

nates) and the albedo ρ. We developed the solution to this system of equations, and employed it in a simple photometric stereo algorithm. We then compared the algorithm with a similar orthographic method on both synthetic and real-life images. The perspective approach gained lower error rates than the orthographic on both synthetic and real images according to all measures. As both algorithms share the same numerical basis (and even the same code for the integration part), we conclude that the transition to a more realistic projection model, the perspective model, is the cause of any improvement.

Acknowledgements: The authors thank Shay Rochel, Tal Darom and Yan Ivanchenko for their technical assistance.

References

[1] S. Barsky and M. Petrou. The 4-source photometric stereo technique for three-dimensional surfaces in the presence of highlights and shadows. *IEEE PAMI*, 25(10):1239–1252, 2003.

[2] R. Basri and D. W. Jacobs. Photometric stereo with general, unknown lighting. In *Computer Vision and Pattern Recognition*, volume 2, pages 374–381, Kauai, Hawaii, Dec. 2001.

[3] F. Courteille, A. Crouzil, J.-D. Durou, and P. Gurdjos. Towards shape from shading under realistic photographic conditions. In *Proceedings of the International Conference on Pattern Recognition*, volume 2, pages 277–280, Cambridge, UK, Aug. 2004.

[4] M. Galo and C. L. Tozzi. Surface reconstruction using multiple light sources and perspective projection. In *International Conference on Image Processing*, pages 309–312, Lausanne, Switzerland, 1996.

[5] B. K. P. Horn. *Robot Vision*. The MIT Press, 1986.

[6] I. Horovitz and N. Kiryati. Depth from gradient fields and control points: Bias correction in photometric stereo. *Image and Vision Computing*, 22(9):681–694, Aug. 2004.

[7] K. Ikeuchi. Determining surface orientations of specular surfaces by using the photometric stereo method. *IEEE PAMI*, 3(6):661–669, November 1981.

[8] K. Ikeuchi. Determining a depth map using a dual photometric stereo. *International Journal of Robotics Research*, 6(1):15–31, 1987.

[9] K. Ikeuchi, H. Nishihara, B. Horn, P. Sobalvarro, and S. Nagata. Determining grasp configurations using photometric stereo and the prism binocular stereo system. *International Journal of Robotics Research*, 5(1):46–65, 1986.

[10] Y. Iwahori, W. Kato, S. Bhuiyan, R. Woodham, and N. Ishii. Neural network based photometric stereo using illumination planning. In *IJCAI97*, pages 1496–1501, 1997.

[11] B. Kim and R. Park. Shape from shading and photometric stereo using surface approximation by legendre polynomials. *CVIU*, 66(3):255–270, June 1997.

[12] R. Kozera. *Existence and Uniqueness in Photometric Stereo*. PhD thesis, Flinders University of South Australia, School of Information Science and Technology, June 1991.

[13] K. M. Lee and C. C. J. Kuo. Shape from photometric ratio and stereo. *Journal of Visual Communication and Image Representation*, 7(2):155–162, 1996.

[14] D. Levin. Mesh-independent surface interpolation. In *Geometric Modeling for Scientific Visualization*, Mathematics and Visualization. Springer-Verlag, 2004.

[15] L. Noakes and R. Kozera. Nonlinearities and noise reduction in 3-source photometric stereo. *Journal of Mathematical Imaging and Vision*, 18(2):119–127, 2003.

[16] T. Okatani and K. Deguchi. On uniqueness of solutions of the three-light-source photometric stereo: Conditions on illumination configuration and surface reflectance. *CVIU*, 81(2):211–226, February 2001.

[17] R. Onn and A. Bruckstein. Integrability disambiguates surface recovery in two-image photometric stereo. *International Journal of Computer Vision*, 5(1):105–113, Aug. 1990.

[18] E. Prados and O. Faugeras. Perspective shape from shading and viscosity solutions. In *International Conference on Computer Vision*, volume 2, pages 826–831, Oct. 2003.

[19] W. H. Press, S. A. Teukolsky, W. T. Vetterling, and B. P. Flannery. *Numerical Recipes in C*. Cambridge University Press, 2nd edition, 1999.

[20] H. Tagare and R. de Figueiredo. A theory of photometric stereo for a class of diffuse non-lambertian surfaces. *Pattern Analysis and Machine Intel.*, 13(2):133–152, Feb. 1991.

[21] A. Tankus, N. Sochen, and Y. Yeshurun. A new perspective [on] Shape-from-Shading. In *Proceedings of the $9^{\underline{th}}$ IEEE International Conference on Computer Vision*, volume II, pages 862–869, Nice, France, Oct. 2003.

[22] A. Tankus, N. Sochen, and Y. Yeshurun. Shape-from-Shading under perspective projection. *International Journal of Computer Vision*, 63(1):21–43, June 2005.

[23] R. Woodham. Determining surface curvature with photometric stereo. In *Proceedings of the Conference on Robotics and Automation*, pages 36–42, Scottsdale, AZ, 1989.

[24] R. J. Woodham. Photometric stereo: A reflectance map technique for determining surface orientation from a single view. In *Image Understanding Systems and Industrial Applications*, volume 155, pages 136–143, San Diego, CA, 1978.

[25] R. J. Woodham. Photometric method for determining surface orientation from multiple images. *Optical Engineering*, 19(1):139–144, 1980.

[26] A. L. Yuille, D. Snow, R. Epstein, and P. N. Belhumeur. Determining generative models of objects under varying illumination: Shape and albedo from multiple images using SVD and integrability. *International Journal of Computer Vision*, 35(3):203–222, Dec. 1999.

[27] R. Zhang, P.-S. Tsai, J. E. Cryer, and M. Shah. Shape from Shading: A survey. *IEEE PAMI*, 21(8):690–705, 1999.